Computational Materials Science 79 (2013) 527–533

Contents lists available at SciVerse ScienceDirect

Computational Materials Science

journal homepage: www.elsevier.com/locate/commatsci

Ab initio calculations for the *F*-center transfer and *R* centers in SrF_2

H. Shi [a,*], L. Chang [a], R. Jia [b], R.I. Eglitis [c]

[a] School of Science, Beijing Institute of Technology, 100081 Beijing, PR China
[b] Department of Mathematics and Natural Sciences, Bergische Universität Wuppertal, D-42097 Wuppertal, Germany
[c] Institute of Solid State Physics, University of Latvia, 8 Kengaraga Str., Riga LV1063, Latvia

ARTICLE INFO

Article history:
Received 17 October 2012
Received in revised form 27 June 2013
Accepted 1 July 2013

Keywords:
DFT
Electronic structure
F center
R center
Band structure

ABSTRACT

We have simulated the *F*-center transfer and *R* center in SrF_2 crystal by using density functional theory (DFT) with a hybrid B3PW description of exchange and correlation. Our calculations show that the *F*-center diffusion barrier is equal to 1.84 eV. During the *F*-center transfer, the trapped electron is more delocalized than that in the regular *F*-center case, and the gap between defect level and conduction bands (CB) in the α-spin state decreases. The formation energy calculations of *R* center show the trend of *F* centers to aggregate in SrF_2. During the *F*-center aggregation, a considerable covalency forms between two neighboring fluorine vacancies with trapped electrons. Three incompletely paired electrons trapped in the *R* center have an up-down-up spin arrangement and induce three defect levels in the gaps between valence bands (VB) and conduction bands for both of α- and β-spin polarized band structures, respectively. More defect bands lead to more complex electron transitions, which were classified into two *F*- and four *M*-like transitions. The DOS calculations clearly reveal the components of defect bands.

1. Introduction

Alkaline-earth fluorides attract considerable attentions due to their wide band gaps, which are larger than 10 eV, making the Alkaline-earth fluorides have a widely use in ultraviolet (UV) region than quartz. As for SrF_2 crystal the experimentally band gap comes to 11.25 eV [1]. Therefore the SrF_2 crystal has more potential in optical applications and it has attracted considerable attentions both in experimental and theoretical studies [2–23].

It is well known that during the generation of the crystals, the defects and impurities may emerged and they strongly affected the optical and mechanical properties of the crystals. As an potential material of the optical application, the SrF_2 crystal is also affected by the internal defects. In order to understand and manipulate the generation of the defects in SrF_2 crystal, some theory research must be done.

The *F* center is one kind of the intrinsic color centers in crystal, in this type of crystallographic defect, the anionic vacancy is filled by one or more electrons which depending on the charge of the missing anion in the crystal. As in SrF_2 crystal, the anionic vacancy missed a fluorine atoms so one electron was trapped by the vacancy. The *F* center in SrF_2 crystal has been studied by den Hartog, Arends, e.g. with electron paramagnetic resonance (EPR) in 1967 [24] and by Stoneham, Hayes, e.g. with Electron Nuclear Double Resonance (ENDOR) in 1968 [25]. We studied the *F* center transfer in SrF_2 crystal in our present work and make an approach of the *R* center in SrF_2 crystal as an extension.

The article is organized as follows: Section 2 makes an introduction of the computational method and first principle calculation details. In Section 3, the defect structure, relaxation of the surrounding atoms, energetic properties and electronic structure of the *F*-center transfer and the *R* centers were discussed. The electron charge and spin density maps, band structures, and DOS plots are illustrated there to help readers to understand the properties of the single *F* center and their aggregations.

2. Calculation method

There are two types about ab initio calculations, one is based on Hartree-Fork (HF) method, the other is based on density functional theory (DFT). As those two method lead to a deviation of the calculation (the first type considerably overestimates the band gap meanwhile the second type underestimates it). So we choose the hybrid exchange–correlation B3PW functional as the base of our ab initio calculations. The hybrid exchange–correlation B3PW functional involving a mixture of nonlocal Fock exact exchange, local-density approximation (LDA) exchange, and Becke's gradient corrected exchange functional [26], combined with the nonlocal gradient corrected correlation potential of Perdew and Wang [27–30]. As in our previously calculations about perfect CaF_2, BaF_2 and SrF_2 crystals, the hybrid DFT-B3PW method gave the best agreement with experiments for the lattice constant, bulk modulus, and optical band gap [6,7]. So as in our present calculations

* Corresponding author. Tel.: +86 010 68916234.
E-mail address: shihongting@gmail.com (H. Shi).

0927-0256/$ - see front matter © 2013 Elsevier B.V. All rights reserved.
http://dx.doi.org/10.1016/j.commatsci.2013.07.001

of the *F*-centers transfer and *R* centers in SrF_2 crystal, we still use the hybrid DFT-B3PW method. Our present calculations were performed by the CRYSTAL-2009 computer code [31]. The CRYSTAL-2009 code employs the Gaussian-type functions (GTF) localized at atoms as the basis for an expansion of the crystalline orbitals. In order to employ the LCAO-GTF (linear combination of atomic orbitals) method, it is desirable to have optimized basis sets (BS). The basis set for the strontium atoms we used in this calculation developed by Habas et al. [32]; for the fluorine atoms, the basis set we used was developed by Nada et al. [33]. We set our supercell with the $3 \times 3 \times 3$ Pack–Monkhorstnet [34], this supercell contains 96 atoms and provides the balanced summation in direct and reciprocal spaces. In consideration of the accuracy of our calculation and the large computational time for the supercell, we set the calculation thresholds *N* (i.e, the calculation of integrals with an accuracy of 10^{-N}) as 7, 7, 7, 7 and 14 for the Coulomb overlap, Coulomb penetration, exchange overlap, the first exchange pseudo-overlap and the second exchange pseudo-overlap, respectively [35]. The lattice constant we used for the SrF_2 bulk is 5.8462 Å.

To simulate *F* and *R* centers, we started with the 96-atom supercell with one or three of the fluorine atoms removed, respectively. After fluorine atoms are removed, the atomic configuration of the surrounding atoms is reoptimized via a search of the total energy minimum as a function of the atomic displacements from the regular lattice sites. In order to have an accurate description of the *F* center, a basis set has been added at the fluorine vacancy (V_F), corresponding to the *ghost* atom. The BS choice of the ghost is optional and the V_F occupies a fluorine site, so we used the same basis set as that used for the fluorine atoms of the perfect SrF2 crystal.

3. Results and discussion

3.1. F-center transfer

The *F* center in SrF_2 (an electron trapped in the fluorine vacancy) is created due to removal of the anion by irradiation or by additive coloration. The geometrical structures, atomic relaxations, energetic properties, and electronic structures, as well as complex electron transitions for the *F*- and *M*-center systems, have been compiled in our previous work [6]. As an extension of our previous study, we performed calculations for the *F*-center transfer between two neighboring atomic sites. According to the crystalline structure of SrF_2, it is obvious that the energetically most favorable *F*-center transfer should be the position switch between the two nearest neighboring fluorine sites, as we can see in Fig. 1. We calculated the energies at several points along the *F*-center transfer path, showing that the corresponding *F*-center diffusion barrier, the highest relative energy during the *F*-center transfer, is equal to 1.84 eV.

The V_F site with trapped electron (*F* center) is surrounded in the ideal lattice by four strontium atoms, forming a tetrahedron, and the next-nearest neighbor shell is formed by six fluorine atoms (see Fig. 1). The calculations of the positions of 10 atoms surrounding the *F* center in SrF_2 with symmetry group T_d after the lattice relaxation to the minimum of the total energy show that attractions of the four nearest Sr atoms from the *F* center by 0.04% of the lattice constant (a_0) and inward displacements of the second-nearest neighbor *F* atoms by 0.27% of a_0 are small, since the effective charge of the *F* center is close to the effective charge of fluorine ions in perfect crystals, indicating that the trapped electron is well localized inside the vacancy. However, the atomic relaxation during the *F*-center transfer is much stronger than that in the regular *F*-center system. Fig. 2a shows the displacements of the surrounding Sr atoms as a function of F0 position. The relaxations increase with the *F*-center transfer and reach approximately 3.60% of a_0 for Sr1, which is a much stronger relaxation than that in the regular *F*-center case. The displacements of Sr2 and Sr3, the other strontium atoms neighboring the *F* center and the F0 atom, also have remarkable shifts of around 0.79% and 1.14% of a_0, respectively, during the *F*-center transfer.

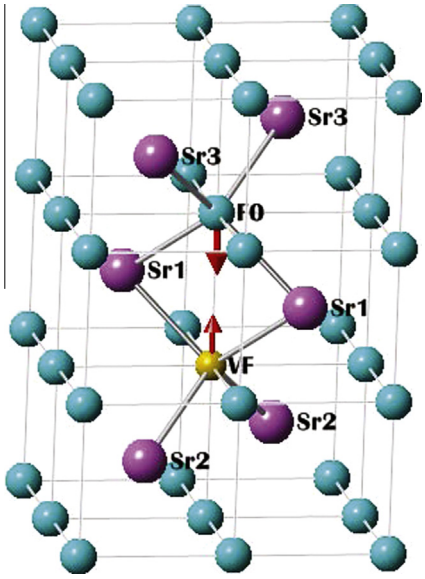

Fig. 1. A view of the *F*-center neighbor geometry in SrF_2, with the indication of *F*-center transfer by arrows. The fluorine atom exchanged with the *F* center is labeled F0, the strontium atoms in different groups are labeled Sr1, Sr2 and Sr3, and V_F is labeled VF. Origin is set at the midpoint between the *F* center and F0.

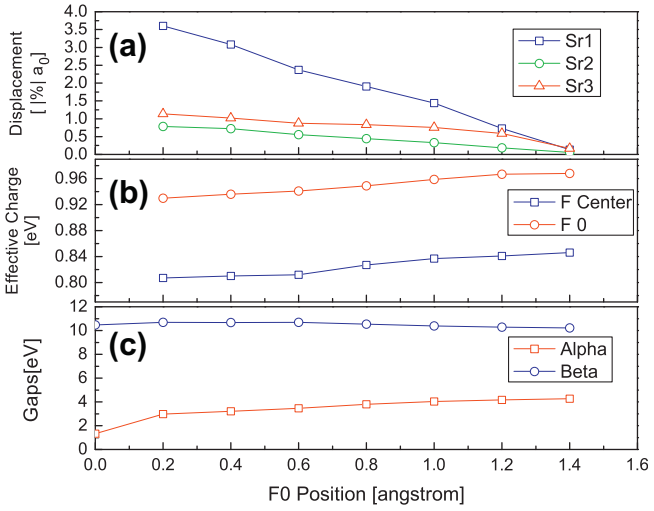

Fig. 2. (a) The displacements of surrounding Sr atoms, (b) effective charges of the *F* center and F0, and (c) gaps of α-CB (the gap between defect band and conduction bands in the α-spin state) and VB-β (the gap between valence bands and defect band in the β-spin state), as a function of F0 position. Sr1, Sr2, Sr3 and F0 are defined in Fig. 1

According to the calculation of the Mulliken effective charge, we found that the electron associated with the removed fluorine atom is well localized (−0.847 e) inside the V_F. With exchanging between the F0 and *F* center, their effective charges decrease, implicating an outward electron transfer, as depicted in Fig. 2b. When F0 approaches the midway of the *F*-center transfer, some part of the trapped electron will be localized on the other side of F0. According to our calculations, the effective charge of −0.086 e is located on the other side of F0, for the F0 location with a coordinate of

0.20 Å. The corresponding values for larger F0-coordinate cases are negligible. For the F0-midway case, the trapped electron (the *F* center) is equally localized (−0.441 e) on both sides of F0 and the effective charge of F0 is −0.856 e, which is much smaller than the fluorine charge of −0.954 e in a perfect SrF_2 crystal.

SrF_2 exhibits an absorption band observed experimentally around 2.85 eV [36]. Our results for defect levels suggest a possible mechanism for explanation of the optical absorption. In the ground state, the defect band is occupied in the α state but is unoccupied in the β state. The optical absorption corresponds to an electron transition from the *F*-center ground state to the conduction band (CB). Because of the spin difference between α and β states and the selection rules, the electron transition from the occupied α band to the unoccupied β band is impossible. The experimentally observed optical absorption could be due to an electron transition from the *F*-center ground state to the CB bottom within the same spin state. Our calculated corresponding value is 4.28 eV, which is reasonable; however, it still is overestimated with respect to the experimental result. It is well known that only the highest occupied one-electron level has a strict physical meaning in exact DFT, which is merely a formalism for the electronic ground state. This discrepancies may be caused by the reason, that we calculated the optical absorption energy as a difference between occupied and unoccupied one-electron energies, which in general is very crude approximation, but could be justified in our case by the fact, that our calculated band gaps are reasonable and close to the experimental value. Additionally, there also should be a possible β-electron transition from the occupied VB top to the unoccupied defect band between the VB–CB gap, and the calculated value of 10.20 eV is considerably larger than the transition in the α-spin case. Fig. 2c shows the calculated variation of band gaps with positions of F0 during the *F*-center transfer. The α-CB gap obviously decreases during the position switching between the F0 and *F* center. When the F0 shifts to the middle position, the α-CB gap is reduced to around 1.33 eV, being much smaller than that in the regular *F*-center case. On the other hand, the variation of the VB-β gap is not remarkable, whereas, unlike the α-CB case, it is not monotonic, and the values are around 10.4 eV, being close to the value of the regular *F*-center case (around 10.2 eV). We conclude that the upward shift of the α-occupied band is notable and the shift of the β-unoccupied band is negligible during the *F*-center transfer. As mentioned before, the electrons trapped in fluorine vacancies form the α-occupied band and the V_F effective charge decreases during the *F*-center transfer; therefore, the upward shift of the α-occupied band could be explained by the fact that the electrons trapped in fluorine vacancies are more delocalized, leading to higher energies.

3.2. R center

As an extension of our study dealing with *F* center in SrF_2 bulk, we performed calculations for more complex *F*-center aggregates, named *R* center which consists of three neighboring *F* centers. Because of the symmetry $Fm\bar{3}m$ of the SrF_2 structure, there are five possible configurations of the *R* center, as in Fig. 3 we can see those five configurations named configs 1, 2, 3, 4 and 5 respectively in this paper. According to our calculations the configs 1 and 2 are the energetically most favorable configurations for *R* centers in SrF_2. The energy difference between them is less than 0.005 eV. Compared to configs 3, 4 and 5, the total energy of config 1 drops by around 0.20 eV, 0.14 eV and 0.20 eV, respectively. Configs 1 and 2 have very close total energies and are more stable than other configurations; therefore, we mainly focus our current discussion on configs 1 and 2. As a starting point of our *R*-center calculations, we computed the formation energy of three neighboring fluorine vacancies. In the supercell calculation for vacancies with trapped electrons, the formation energy of a neutral (the total charge of the supercell is zero) *R* center in SrF_2, could be expressed as follows:

$$E^{(R)}_{\text{formation}} = E(\text{Fluorine}) \times 3 + E(R) - E(\textit{perfect}) \quad (1)$$

where E(Fluorine) is the energy for an isolated fluorine atom, $E(R)$ is the total energy of the defective crystal containing an *R* center and E(perfect) is the total energy of the perfect crystal. Our calculation results for the formation energy of configs 1 and 2 are 23.52 eV and 23.51 eV, respectively. The formation energies of these two configurations are almost the same, and they are smaller than 3 times of the *F*-center formation energy (7.98 eV × 3) by around 0.43 eV. It means that the formation of the complex of three aggregated *F* centers is easier than the formation of three separated *F* centers. Here, we can define the association energy of three *F* centers as the energy difference between the same three remote *F* centers and the *R* center, and the corresponding value is + 0.43 eV. With this definition, the positive sign indicates stable aggregation. In our previous *M*-center study, a considerable covalent bond forms between two *F* centers after their aggregation; therefore, we can consider the association energy of two *F* centers as the *F*-bond energy. For *R*-center configs 1 and 2, there are two *F*-bonds in each *R* center, so it is reasonable that the *F*-center-aggregated system is more stable than the system consisting of the separated *F* centers.

Figs. 4 and 5 depict the geometry relaxations of the strontium atoms surrounding the *R* center. For config 1, the four Sr1 atoms are repulsed from the V_{F1} by around 0.36% of a_0, and the four Sr2 atoms are attracted from the V_{F2} by around 0.16% a_0, as we can see in Fig. 4. As a whole, according to our calculations, there are no displacements over 0.4% of a_0 for atoms surrounding the *R* center in config 1. However, for config 2, the relaxation of the *R*-center system is slightly stronger. The nearest Sr atoms labeled Sr1, Sr2, Sr3 and Sr4 are repulsed from the *R* center by around 0.21%, 0.60%, 0.26% and 0.19% of a_0, respectively, and the two Sr5 atoms move toward the *R* center by around 0.29% of a_0 (see Fig. 5). From our calculated relaxations of the nearest strontium atoms in the *F*- and *R*-center systems, we found that the displacements of the strontium atoms with one or two nearest V_F are small and less than

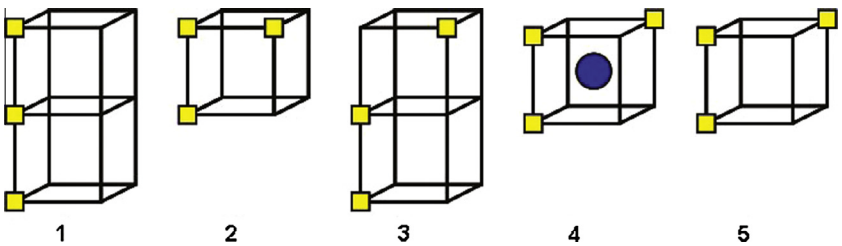

Fig. 3. Schematic sketch of five different *R*-center configurations. Fluorine vacancies are denoted by squares. Configurations are labeled 1, 2, 3, 4, and 5 from left to right ordinally. The blue circle indicates a strontium atom located at the center of the cubic formed by eight fluorine atoms.

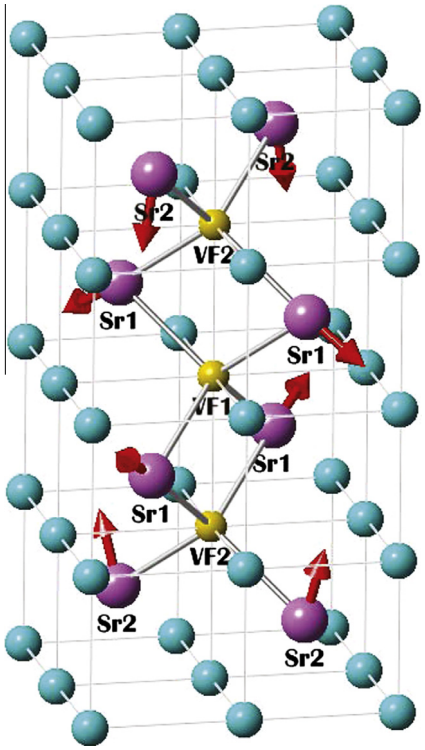

Fig. 4. A view of the *R*-center neighbor geometry in SrF_2, with the indication of relaxation shifts for config 1. The nearest strontium atoms in inequivalent groups are labeled Sr1 and Sr2, respectively.

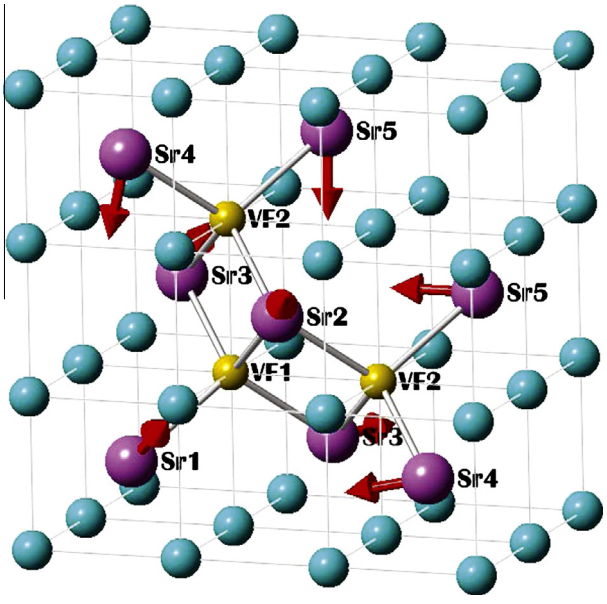

Fig. 5. A view of the *R*-center neighbor geometry in SrF_2, with the indication of relaxation shifts for config 2. The nearest strontium atoms in inequivalent groups are labeled Sr1, Sr2, Sr3, Sr4 and Sr5, respectively.

0.4% of a_0, and for the strontium atom labeled Sr2 in *R*-center config 2, containing three nearest V_F with trapped electrons, the shift reaches around 0.6% of a_0. It implicates that the relaxation of the strontium atoms surrounding the *R* center has a quasi-superposition effect. The Sr atoms having more nearest V_F exhibit stronger relaxations. Additionally, all the shifts of the surrounding strontium atoms in the *R* center (0.16–0.60% of a_0) are much larger than that in the *F*-center case (0.04% of a_0).

Table 1
The effective charges (Q (e)) of the *R* center and surrounding atoms in SrF_2, for an 96-atom supercell. ΔQ (e) is the charge difference between the defective and perfect crystals (Q_{Sr} = +1.919 e, Q_F = −0.954 e in perfect SrF_2). Spin is the result of the spin difference of electrons with different spin directions ($n_\alpha - n_\beta$) also in unit (e).

	Atoms (*shell*)	Number	Q (e)	ΔQ (e)	Spin (e)
Config 1	V_{F1}	1	−0.862	+0.092	−0.550
	V_{F2}	2	−0.869	+0.085	+0.667
	Sr1	4	+1.910	−0.009	+0.002
	Sr2	4	+1.904	−0.015	+0.018
Config 2	V_{F1}	1	−0.858	+0.096	−0.546
	V_{F2}	2	−0.870	+0.084	+0.674
	Sr1	1	+1.904	−0.015	−0.015
	Sr2	1	+1.915	−0.004	+0.021
	Sr3	2	+1.909	−0.010	+0.003
	Sr4	2	+1.904	−0.015	+0.018
	Sr5	2	+1.904	−0.015	+0.019

Table 1 shows the effective charge and spins of the *R* center and surrounding strontium atoms for config 1 and 2. Obviously, the fluorine vacancies V_{F1} and V_{F2} are not equivalent for the *R*-center systems. For config 1, the effective charges of V_{F1} and V_{F2} are −0.862 and −0.869 e, respectively. The average charge of three fluorine vacancies is equal to −0.867 e, being more localized inside the *R* center with respect to the *F*-center case (−0.848 e). Around 0.096 e from the eight neighboring strontium atoms transfers toward the *R* center, and according to our calculation, some charges belonging to the nearest fluorine atoms also shift to the *R* center. For config 2, the average charge of three V_F (−0.866 e) is close to the corresponding value of config 1, and also is more localized than that in the *F*-center case. Bond population calculations for the *R*-center systems show that there is a considerable covalency between V_{F1} and V_{F2}, 148 and 156 *me* for configs 1 and 2, respectively. Nevertheless, they are much weaker than in the *M*-center case (268 *me*). These weaker covalencies in the *R*-center systems can be explained by the fact that the electrons localized on V_{F1} and V_{F2} are not completely paired. However, we can still conclude that there are two considerable covalencies in each *R* center. The charge density maps of the *R* center for configs 1 and 2 are displayed in Fig. 6, also showing that the V_F charges are well localized inside the *R* center and the deformation of the neighboring ions from their spherical shapes is negligible.

Because there are three V_F in one *R* center, not all electrons inside the V_F can be paired. The localization of the unpaired electron in the *R* center is clearly shown in the spin density map and the spin polarization of the nearest neighboring atoms is also appreciable, as we can see in Fig. 6. From Fig. 6, we can see that the spin polarizations of the nearest atoms are remarkable and the spin densities between V_{F1} and V_{F2} almost disappear, reflecting the presence of paired electron distributions. We define the spin of the *R* center as the sum of three V_F spins. For config 1, the *R*-center spin is +0.784 e, which is close to that of the *F*-center case (+0.797 e). The V_{F1} (−0.550 e) and V_{F2} (+0.667 e) spins have opposite signs, and the arrangement of V_F spins has a (↑↓↑) style. The *R*-center spin for config 2 is equal to +0.802 e and is bigger than that of config 1. The $V_{F2} - V_{F1} - V_{F2}$ with the spins of +0.674, −0.546 and +0.674 e respectively, also have a (↑↓↑) style.

We also calculated the band structures of the *R* centers in SrF_2, crystals (see Fig. 7). The optical band gaps for configs 1 and 2 are collected in Table 2. Because of the presence of an unpaired electron in the *R* center, the band structure is polarized. Three fluorine vacancies induce three α- and three β-bands in the VB-CB gaps, two α- and one β-bands labeled α_1, α_2 and β_1 are occupied, and one α- and two β-bands labeled α_3, β_2 and β_3 denote empty vacancy levels, as we can see in Fig. 7. The (↑↓↑) spin style of the *R* center mentioned before also demonstrates that there should be two and

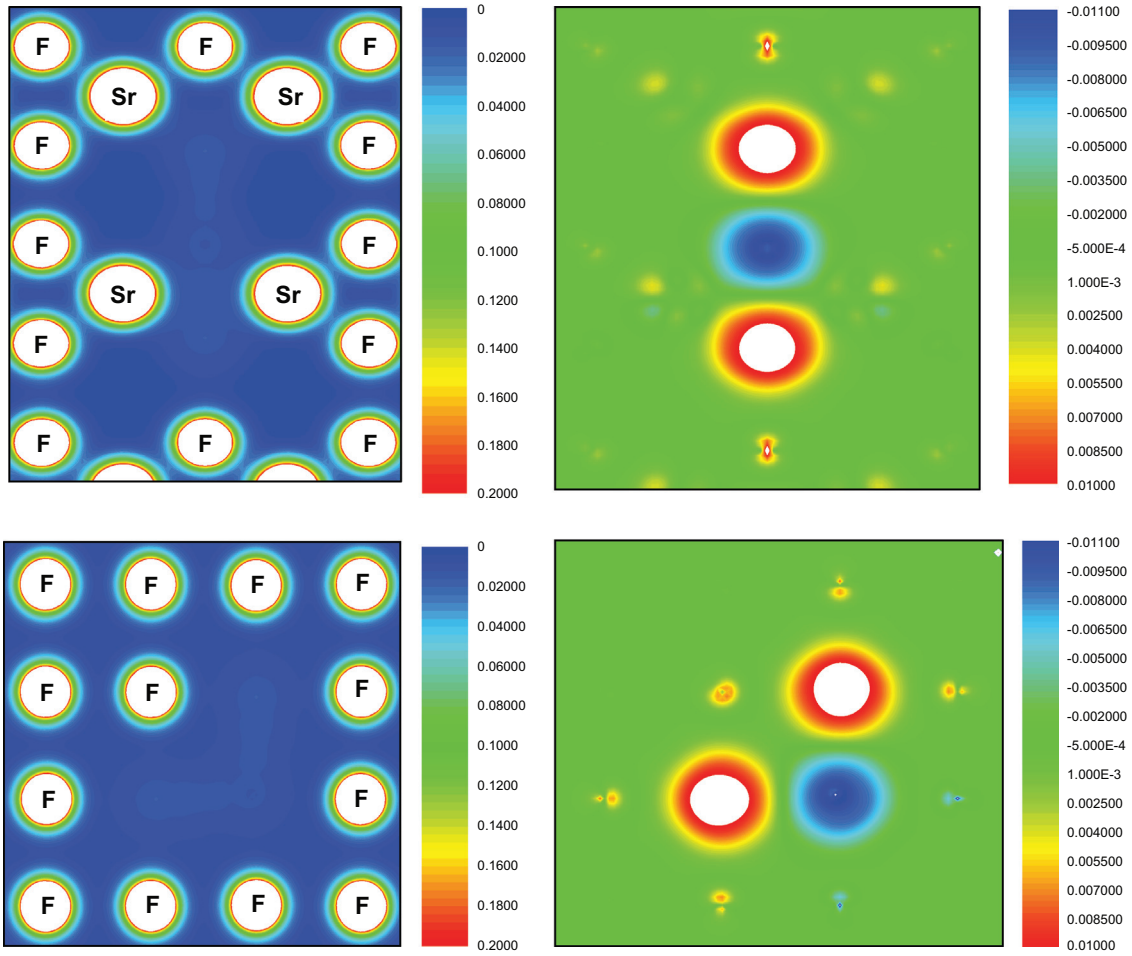

Fig. 6. Electron density (left) and spin density (right) contours in SrF_2. being from 0 to 0.2 e/bohr^3 with a linear increment of 0.002 e/bohr^3 and from −0.011 to 0.01 e/bohr^3 with a linear increment of 3×10^{-4} e/bohr^3, respectively. The upper and lower maps indicate the config 1 and 2, respectively.

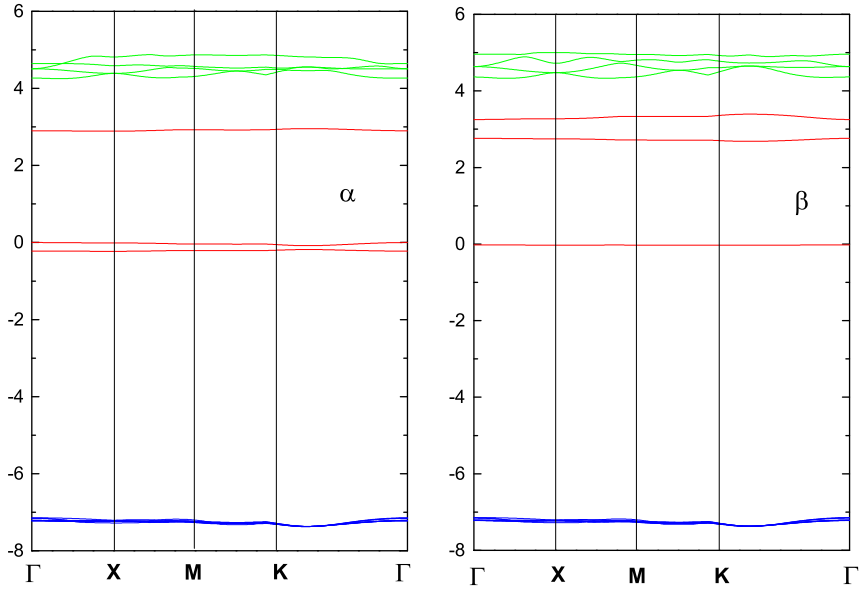

Fig. 7. Calculated B3PW band structure of the 96-atom supercell modeling the *R* center in SrF_2, for config 1. α and β denote the up- and down-spin bands, respectively. Fermi energy is shifted to zero eV.

Table 2
Direct optical band gaps (eV) ($\Gamma \rightarrow \Gamma$) for *R*-center systems in configs 1 and 2.

	Gaps	Config 1	Config 2
α-spin	$\alpha_1 \rightarrow \alpha_3$	3.12	3.24
	$\alpha_2 \rightarrow \alpha_3$	2.90	2.80
	$\alpha_1 \rightarrow$ CB	4.49	4.44
	$\alpha_2 \rightarrow$ CB	4.27	4.25
β-spin	$\beta_1 \rightarrow \beta_2$	2.78	3.08
	$\beta_1 \rightarrow \beta_3$	3.27	3.13
	$\beta_1 \rightarrow$ CB	4.38	4.25

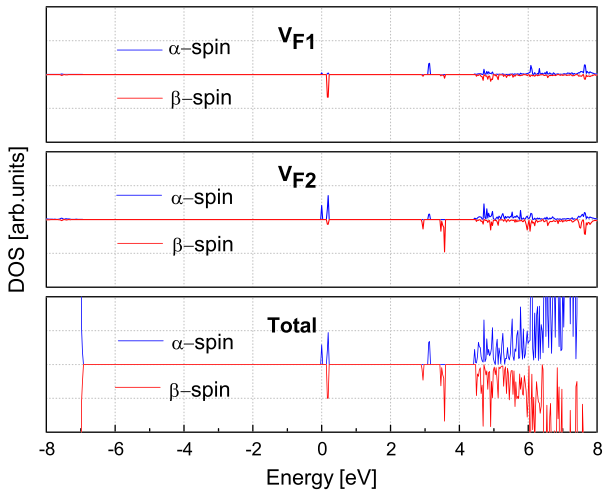

Fig. 8. Total and partial density of states (DOS) for the *R*-center in config 1. α and β denote the up- and down-spin states, respectively. Fermi energy is shifted to zero eV.

one occupied defect bands in the α and β states, respectively, being in accordance with the band structure calculations. According to the selection rules, the $\alpha \rightarrow \beta$ transition is forbidden, and we can summarize that the electron transitions in the *R*-center systems have the following possibilities: $\alpha_1 \rightarrow \alpha_3$, $\alpha_2 \rightarrow \alpha_3$, $\alpha_1 \rightarrow$ CB, $\alpha_2 \rightarrow$ CB, $\beta_1 \rightarrow \beta_2$, $\beta_1 \rightarrow \beta_3$, $\beta_1 \rightarrow$ CB, and the corresponding values are listed in Table 2. We may classify these electron-transition ways into two categories, the four ways of $\alpha_1 \rightarrow \alpha_3$, $\alpha_2 \rightarrow \alpha_3$, $\beta_1 \rightarrow \beta_2$ and $\beta_1 \rightarrow \beta_3$ belong to the *M*-like optical absorption, namely, the transition from the defect occupied band to a defect unoccupied level, similar to the electron-transition way in *M*-center systems, and the three ways of $\alpha_1 \rightarrow$ CB, $\alpha_2 \rightarrow$ CB and $\beta_1 \rightarrow$ CB express the *F*-like optical absorption, corresponding to the transition from the defect occupied state to CB. Here, we can consider an *R* center as a combination of two *M* centers having one common V_F or of three *F* centers; therefore, the two *M* centers contribute to the four *M*-like optical absorptions, and the three *F* centers introduce the three *F*-like electron transitions. Thus, from Table 2, we can see that the *M*- and *F*-like gaps are comparable to the relevant *M*- and *F*-center gaps, respectively, despite that the *M*-like gaps are larger than the *M*-center gap of 1.93 eV. Unfortunately, we did not find any experimental results for *R* centers in SrF_2, in literatures.

To further study the electronic structure and the electron transitions in an *R*-center system, we calculated the density of states (DOS) of the *R*-center system. The total and projected DOS of *R* centers in SrF_2, are displayed in Fig. 8. We can conclude that the V_{F2}-s orbitals do the major contribution to the occupied bands named α_1 and α_2 and the unoccupied bands named β_2 and β_3, and the occupied band labeled β_1 and the empty level labeled α_3 mainly consist of the V_{F1}-s orbitals, which is in agreement with the former spin density discussion regarding the *R*-center spin arrangement.

4. Conclusions

We preformed our first-principle calculations based on the hybrid DFT-B3PW scheme for the *F*-center transfer and *R* centers in SrF_2 crystal. The structure of SrF_2, crystal implies that the *F*-center transfer should be the position switch between the two nearest neighbor fluorine sites, and this transfer, according to our calculation, requires overcoming an approximately 1.84 eV high energy barrier. During the transfer, the surrounding atoms have a larger relaxation than that in the regular *F*-center system, and the effective charge of the *F* center and F0 decrease. With the position exchanging between the *F* center and F0, the α-CB gap is considerably reduced to 1.33 eV, but the VB-β gap has no obvious change with respect to the regular *F*-center case.

To further understand *F*-center aggregation, we studied a more complex case, namely, *R* center composed of three neighboring *F* centers, by means of the hybrid B3PW method. Several *R*-center configurations were investigated, and we found that configs 1 and 2 (see Fig. 3) are the energetically most favorable configurations for 3-V_F systems. The association energy of three *F* centers in config 1 is +0.43 eV, implicating a trend for the *F* centers to form aggregates. Bond population analysis shows that there are two considerable covalencies between the V_{F1} and V_{F2} in each *R* center, whereas they are much weaker than in the *M*-center case. This weaker covalency in the *R*-center cases can be explained by the fact that the electrons localized on V_{F1} and V_{F2} are not completely paired. The *R* center has a ($\uparrow\downarrow\uparrow$)-style spin. The band structure of the *R* center indicates that there are three defect levels induced by three fluorine vacancies in the VB $\rightarrow$ CB gaps for both α- and β-spin band structures. Several complex electron transitions, namely, $\alpha_1 \rightarrow \alpha_3$, $\alpha_2 \rightarrow \alpha_3$, $\alpha_1 \rightarrow$ CB, $\alpha_2 \rightarrow$ CB, $\beta_1 \rightarrow \beta_2$, $\beta_1 \rightarrow \beta_3$, $\beta_1 \rightarrow$ CB, are classified into *F*- and *M*-like transitions. The analysis of DOS calculations clearly indicates that the V_{F2}-s orbitals mainly form the occupied α_1 and α_2 bands and the unoccupied β_2 and β_3 bands, and the V_{F1}-s orbitals do the major contribution to the occupied β_1 band and the empty α_3 band.

Acknowledgments

H. Shi was supported by NSFC Grant No. 11004008. R. I. Eglitis was supported by ESF Grant No. 2009/0202/1DP/1.1.1.2.0/APIA/VIAA/141.

References

[1] G.W. Rubloff, Physical Review B 5 (1972) 662.
[2] S.C. Yoo, H.B. Radousky, N.C. Holmes, Physical Review B 44 (1991) 830.
[3] J.J. Tu, A.J. Sievers, Physical Review Letters 83 (1999) 4077.
[4] K. Inoue, N. Suzuki, T. Hyodo, Physical Review B 71 (2005) 134305.
[5] T. Kohmoto, Y. Fukuda, M. Kunitomo, K. Isodo, Physical Review B 62 (2000) 579.
[6] R. Jia, H. Shi, G. Borstel, Computational Materials Science 43 (2008) 980–988.
[7] L. Yue, R. Jia, H. Shi, et al., Journal Physics Chemistry A 114 (2008) 8444–8449.
[8] K. Schmalzl, D. Strauch, H. Schober, Physical Review B 68 (2003) 144301.
[9] N.H. de Leeuw, T.G.J. Cooper, Materials Chemistry 13 (2003) 93.
[10] N. Leeuw, H. Purton, J.A. Parker, S.C. Watson, G.W. Kresse, G. Surf, Science 452 (2003) 9.
[11] J. Kudrnovsky, N.E. Christensen, J. Masek, Physical Review B 43 (1991) 12597.
[12] M. Verstraete, X. Gonze, Physical Review B 43 (2003) 195123.
[13] J. Barth, R.L. Johnson, M. Cardona, D. Fuchs, A.M. Bradshaw, Physical Review B 41 (1990) R3219.
[14] I. Nepomnyashchikh, E.A. Radzabov, A.V. Egranov, V.F. Ivasheckin, A.S. Istomin, Radiation Effects and Defects in Solids 157 (2002) 715.
[15] A.S. Foster, C. Barth, A.L. Shluger, R.M. Nieminen, M. Reichling, Physical Review B 66 (2003) 7.
[16] M. Merawa, M. Lunell, R. Orlando, M. Gelize-Duvignau, R. Dovesi, Chemical Physics Letters 368 (2003) 7.
[17] A.V. Puchina, V.E. Puchin, E.A. Kotomin, M. Reichling, Solid State Communications 106 (1998) 285.
[18] M. Catti, R. Dovesi, A. Pavese, V.R. Saunders, Journal of Physics: Condensed Matter 3 (1997) 4151.

[19] A. Jockisch, U. Schroder, F.W. Wette, W. Kress, Journal of Physics: Condensed Matter 5 (1993) 5401.
[20] Andrey Mysovsky, Evgeny Radzhabov, IEEE Transactions on Nuclear Science 57 (2010) 3.
[21] Himadri R. Soni, Sanjeev K. Gupta, Mina Talati, Prafulla K. Jha, Journal of Physics and Chemistry of Solids 72 (2011) 934–939.
[22] J.S. Wang, C.L. Ma, D. Zhou, Y.S. Xu, et al., Journal of Solid State Chemistry 186 (2012) 231–234.
[23] M. Dreger, G. Scholz, E. Kemnitz, Solid State Sciences B 14 (2012) 528–534.
[24] H.W. den Hartog, J. Arends, Physica Status Solidi (b) 23 (1967) 713.
[25] SA.M. Stoneham, W. Hayes, P.H.S. Smith, J.P. Scott, Proceedings of the Royal Society of London Series A 306 (1968) 369.
[26] A.D. Becke, Journal of Chemical Physics 98 (1993) 5648.
[27] J.P. Perdew, Y. Wang, Physical Review B 33 (1986) 8800.
[28] J.P. Perdew, Y. Wang, Physical Review B 40 (1989) 3399.
[29] J.P. Perdew, Y. Wang, Physical Review B 45 (1992) 13244.
[30] H. Shi, R.I. Eglitis, G. Borstel, Physical Review B 72 (2005) 045109.
[31] R. Dovesi, V.R. Saunders1, C. Roetti, R. Orlando, C. M. Zicovich-Wilson, F. Pascale, B. Civalleri, K. Doll, N.M. Harrison, I.J. Bush, Ph. DArco, M. Llunell, CRYSTAL-2009 User Manual, University of Torino, Italy, 2010.
[32] M.P. Habas, R. Dovesi, A. Lichanot, Journal of Physics: Condensed Matter 10 (1998) 6897–6909.
[33] R. Nada, C.R.A. Catlow, C. Pisani, R. Orlando, Modelling and Simulation in Materials Science and Engineering 1 (1993) 165–187.
[34] H.J. Monkhorst, J.D. Pack, Physical Review B 13 (1976) 5188.
[35] Ouantum-mechanical Ab initio calculations of the properties of crystalline materials, in: PisaniC (ed.), Lecture Notes in Chemistry, vol. 97, Springer-Verlag Berlin, Germany, 1996.
[36] B.C. Cavenett, W. Hayes, I.C. Hunter, A.M. Stoneham, Proceedings of the Royal Society of London Series A 309 (1969) 3.